Received: 17 May 2018 | Revised: 31 July 2018 | Accepted: 13 August 2018

DOI: 10.4218/etrij.2018-0245

ORIGINAL ARTICLE

WILEY ETRI Journal

High-gain polarization conversion metasurface

Aixin Chen | **Xiangwei Ning** | **Xin Liu** | **Zhe Zhang**

School of Electronic and Information Engineering, Beihang University, Beijing, China.

Correspondence
Aixin Chen, School of Electronic and Information Engineering, Beihang University, Beijing, China.
Email: axchen@buaa.edu.cn

Funding information
This research was supported by the National Natural Science Foundation of China (No. 61371006), the Equipment Advance Research Project, the Defense Industrial Technology Development Program, and the Chinese Government Fund.

A novel analytical method based on the cavity mode theory to design a metasurface (MS) is proposed in this study. We carefully analyzed the phase and amplitude characteristics of the incident wave and transmitted wave, and successfully designed a circular polarization conversion MS by introducing a cutting structure with wider operation bandwidth and higher radiation direction gain compared with that of the original MS. For the measurements, a microstrip antenna operating at 2.4 GHz was used as the source antenna to verify the designed MS. The simulation and measurement results agree well with each other.

KEYWORDS
amplitude adjustment, metasurface, phase adjustment, polarization conversion

1 | INTRODUCTION

Metasurfaces (MS) are popular two-dimensional metamaterials [1] that have a thickness much smaller than their wavelength. Based on the generalized Huygens principle, the design of an artificial nonhomogeneous structure at subwavelength scales can realize arbitrary electromagnetic phase distribution. Therefore, it can flexibly and effectively control some electromagnetic characteristics, such as radiation pattern [2], polarization mode [3–6], and transmission mode, to meet specific requirements about antennas. Currently, MS are employed in many applications such as smart surfaces [7], terahertz devices [8,9], fluid control surfaces [10], bandwidth enhancement, [11] and so on.

In recent years, precise propagation control for electromagnetic waves has been a fundamental factor in achieving most breakthroughs in the antenna field. Traditional methods include exploiting antenna arrays and the use of zero-index metamaterials [12] to control electromagnetic waves. However, these methods have intrinsic limitations in the microwave region. For antenna arrays, an extremely complicated feeding network and a large number of antennas may result in challenges in integration with other equipment. For zero-index metamaterials, a certain thickness is usually required to reach several wavelengths, which is necessary for good performance, and inevitably, it results in high values in both weight and volume [13]. MS can overcome these shortcomings owing to its intrinsic properties.

To efficiently design an MS with good performance, there are two general theories: The first theory uses periodic boundary conditions and exact numerical methods. The second theory involves introducing abrupt phase discontinuities on a surface based on generalized laws of reflection and refraction to design an anomalous refraction surface. In [14], this method was proved through various case studies on MS design. In addition, in [15], a microwave RCS reduction structure was designed using an antarafacial reflection design of the gradient MS. We also use this method to prove the advantages of the proposed MS.

These two theories are effective to design and analyze MS. However, they are quite complex and difficult to understand. Therefore, in this study, we propose another efficient and intuitive method based on the cavity mode theory to analyze and design MS. Electromagnetic wave

propagation between the MS and source antenna can be analyzed using the cavity mode theory; then, we can use the results to design an MS.

In Section 2, the cavity mode theory is presented and demonstrated how it can be used to analyze the proposed MS structure to achieve polarization conversion. In Section 3, the phase differences are analyzed and the cutting structure is introduced to the MS. In Section 4, discussion on how to expand the function frequency band and improve the gain is given. In Section 5, details of the experiment are given, and the simulation and measurement results obtained are discussed. In section 6, the conclusions obtained are presented.

2 | ANALYSIS OF METASURFACE THROUGH CAVITY MODE THEORY

Some MS can realize polarization conversion, an example of such an MS is shown in Figure 1. Using this MS, the linear polarization of an incident electromagnetic wave can be transformed into a circular one [16].

We use the cavity mode theory to analyze the proposed MS unit structure and prove that diagonal excitation can achieve polarization conversion. In our analysis, the spatial space between the MS and the source antenna is regarded as a cavity resonator. The electric field can be expressed as a function of the mode ψ_m:

$$E_z = \sum_{m=0}^{\infty} \alpha_m \psi_m(x,y), \tag{1}$$

$$\alpha_m = \frac{jk_0\eta_0}{k^2-k_m^2}\cdot\frac{\int J\Psi_m^* d_s}{\int \Psi_m \Psi_m^* d_s} = \frac{\varphi_m(x',y')}{k^2-k_m^2}. \tag{2}$$

In these functions, m denotes the resonant mode of the united serial number based on the resonance frequency of high and low orders; k_0 is the free space wave number; η_0 is the free space wave impedance; k_m is the resonance wave numbers for the number m mode; J is the excitation current along the Z-axis; and x', y' indicates the position of the excitation current in the unit of MS.

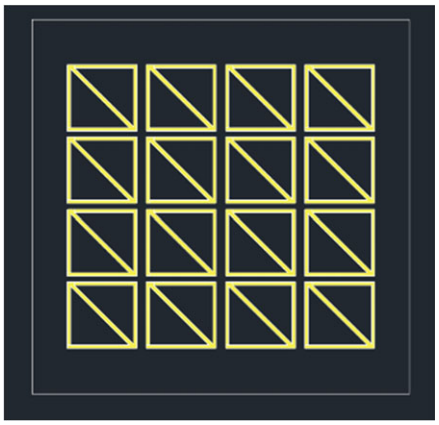

FIGURE 1 Linear-to-circular polarization conversion MS

When the excitation frequency is near the frequency of the m mode, the mode is much stronger than all other modes. Assuming the mode in the Z-axis direction of the far-field radiation field along the X-direction, we have:

$$E_x = jk_0F_m.x = G_m\Phi_m(x',y')/\left(k^2,k_m^2\right). \tag{3}$$

If k_{m+1} is near k_m and $k_m < K' < k_{m+1}$, then the mode of $m+1$ can be excited; in addition, the mode is orthogonal to E_x, as shown by:

$$E_y = jk_0F_{m+1}.y = G_{m+1}\Phi_{m+1}(x',y')/\left(k^2,k_{m+1}^2\right), \tag{4}$$

$$\frac{E_y}{H_x} = \frac{G_{m+1}\Phi_{m+1}(x',y')}{G_m\Phi_m(x',y')}\frac{(k^2-k_m^2)}{\left(k^2-k_{m+1}^2\right)} \approx A\frac{k-k_m}{k-k_{m+1}}, \tag{5}$$

$$A = \left[\frac{G_{m+1}\Phi_{m+1}(x',y')}{G_m\Phi_m(x',y')}\right] \approx \Phi_{m+1}(x',y')/\Phi_m(x',y'). \tag{6}$$

The circular polarization condition is:

$$A = \frac{k-k_m}{k-k_{m+1}} = \pm j. \tag{7}$$

Further,

$$\frac{E_y}{E_X} = \pm j \tag{8}$$

where, $+j$ refers to the left-hand circular polarization (LHCP) and $-j$ refers to the right-hand circular polarization (RHCP).

Because the MS unit is quite similar to a square structure, $k_{10} = \frac{\pi}{a} \approx k_{01} = \frac{\pi}{b}$ can be fulfilled.

Thus,

$$A = \cos(\pi y'/b)/\cos(\pi x'/a), \tag{9}$$

$$\frac{A(k-k_{01})}{k-k_{10}} = \pm j. \tag{10}$$

To obtain the RHCP, the phase of $k-k_{01}$ should be delayed by $\frac{\pi}{2}$ relative to $k-k_{10}$.

The above condition is described in the following function as:

$$A^2 - 2\left(\frac{a}{b}-1\right)QA + \frac{a}{b} = 0 \tag{11}$$

where Q is the Q-factor of the equivalent cavity resonator.

Consider one of the cases: $A_1 = A_2 = 1$; equally, $\frac{y'}{x'} = \frac{b}{a}$. Thus, this result proves that a circular polarization wave can be produced by diagonal excitation.

The design in [16] confirms these formulas, which proves the accuracy of the cavity mode theory analysis. The proposed design of MS can achieve linear-to-circular polarization by adding diagonal excitation.

3 | PHASE ADJUSTMENT AND POLARIZATION CONVERSION WITH FREQUENCY BAND EXPANSION

By simulating the MS shown in Figure 1, we obtain the phases of the incident and transmitted waves. Through phase analysis, the phase difference fluctuation, which is caused by floating the transmission wave phase, occurs as shown in Figure 2.

We introduce the cutting structure to eliminate the phase difference fluctuation and expand the function bandwith of the MS. The cutting structure performs the function of loading the parasitic capacitance shown in Figure 3.

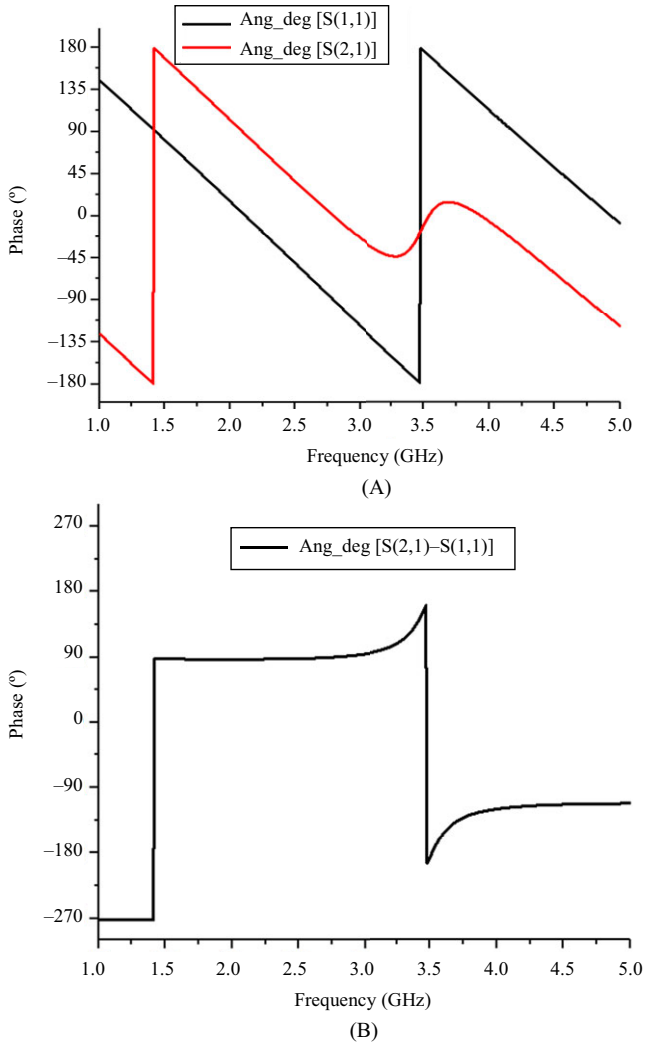

FIGURE 2 (A) Phase of the incident and transmitted waves and (B) phase difference in the incident and transmitted waves

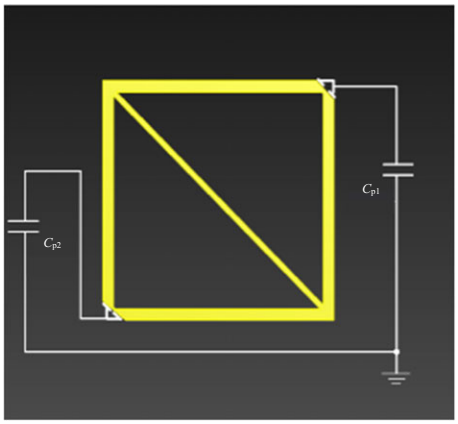

FIGURE 3 Cutting structure with parasitic capacitance

The structure of the MS with the cutting structure is shown in Figure 4. The dimensions of the unit are listed in Table 1. By simulating the electric field distribution of the metal layer of the MS, we obtain two electric field modes and express them as shown in Figure 4(b).

The function of the cutting structure must be analyzed from the perspective of the circuit. As is shown in Figure 3, the value of C_{p1} and C_{p2} can be changed by adjusting the size of the cutting structure. Furthermore, the phase of $\vec{E}_1$ and $\vec{E}_2$ can also changed. A good phase response can be obtained by using a suitable cutting structure design. The results are shown in Figure 5A and B.

From Figure 5, it can be seen that the phase adjustment introduced by the cutting structure helps optimize the polarization conversion effect. The bandwidth is expanded from 1 GHz to 3 GHz, as shown in Figure 2B to 1 GHz to 5 GHz, as shown in Figure 5B which satisfies the absolute value of the phase difference, 90°; this implies the circular polarization conversion bandwidth of the MS is expanded.

4 | AMPLITUDE ADJUSTMENT AND HIGH-GAIN OF THE MS

The phase difference and transmission coefficient with and without the cutting structure are shown in Figure 6.

Figure 6(b) shows that cutting at the area where electric field distribution is relatively concentrated can significantly improve the transmission coefficient.

Taking the MS as a single structure, and assuming that the incident electric field is E_i, the calculation of the energy transfer efficiency η is given as:

$$\eta = \frac{P_{\text{rad}}}{P_I} = \frac{\iint S_r d_s}{\iint S_i d_s} = \frac{\frac{1}{2}\text{Re}\iint \vec{E}_r \times \vec{H}_r d_s}{\frac{1}{2}\text{Re}\iint \vec{E}_I \times \vec{H}_I d_s}, \quad (12)$$

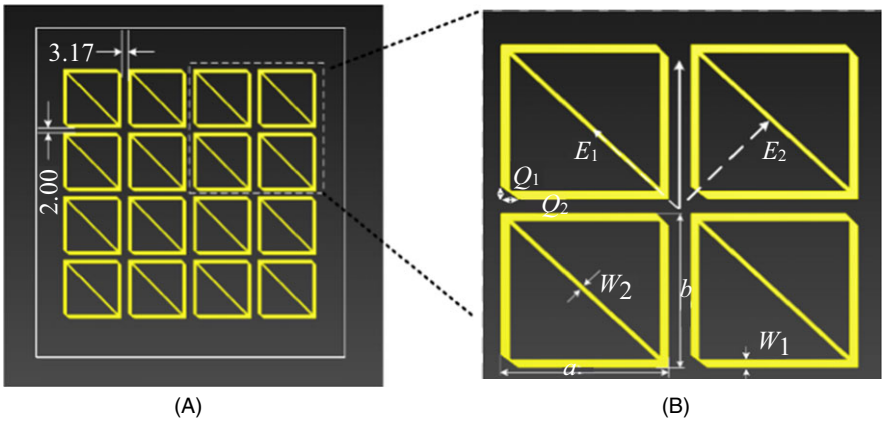

FIGURE 4 (A) Integral structure of MS with the cutting structure and (B) four units extracted for analysis

TABLE 1 Dimensions of the MS unit. (unit: mm)

W_1	W_2	a	b	Q_1	Q_2
2.1	0.46	23.12	22.05	2.9	1.8

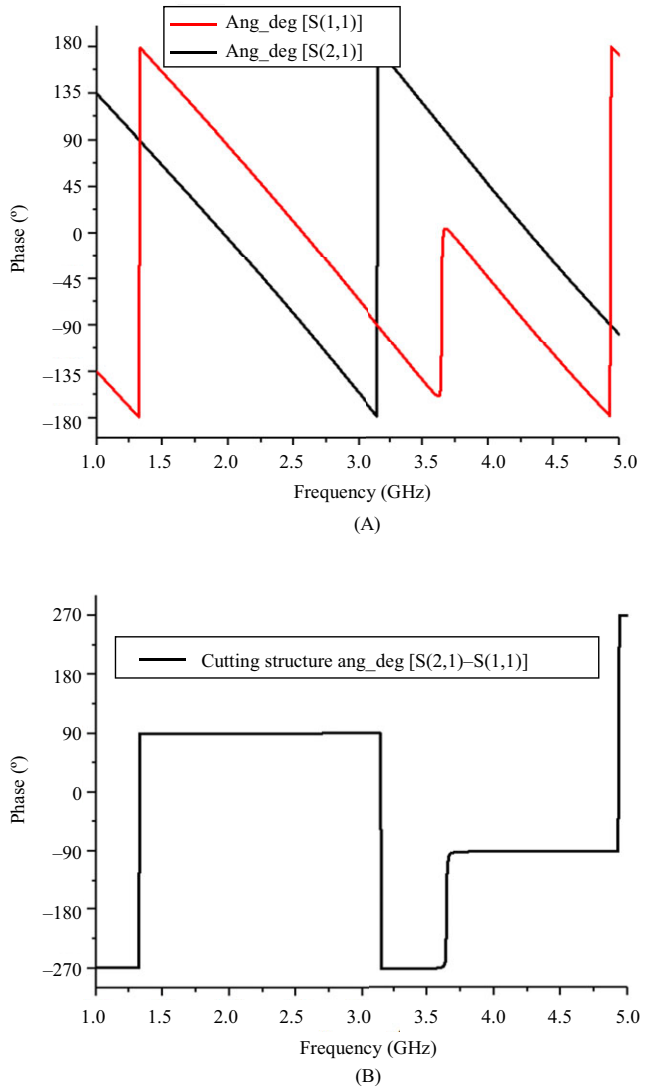

FIGURE 5 (A) Phases of the incident and transmitted waves and (B) phase difference

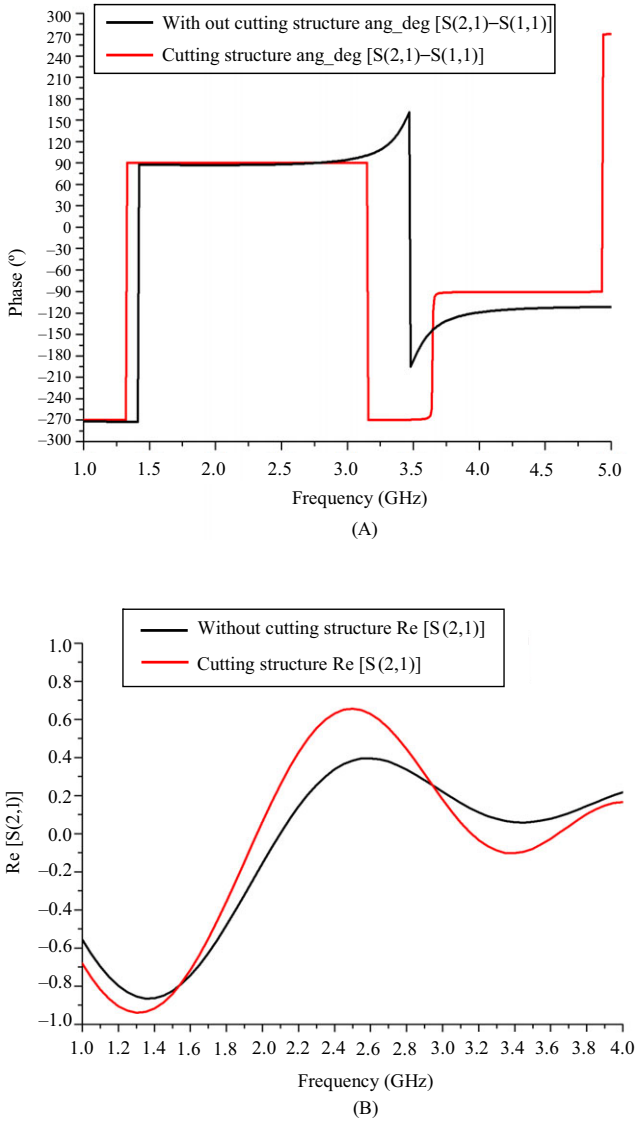

FIGURE 6 (A) Phase difference with and without the cutting structure and (B) Re[S(2,1)] with and without the cutting structure

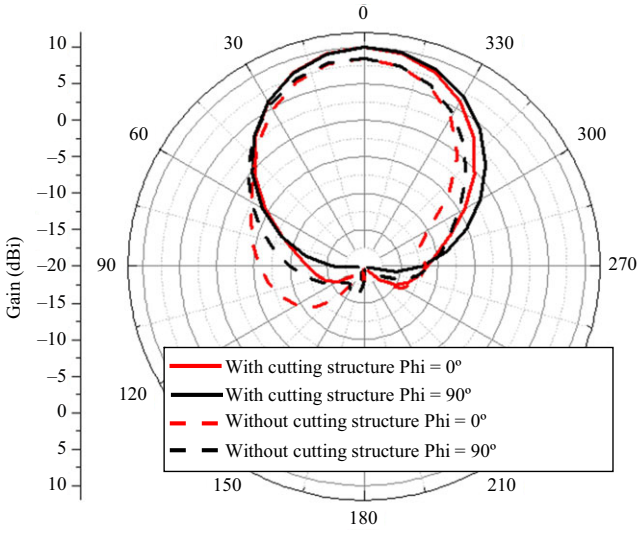

FIGURE 7 Comparison of the gain without and with cutting structure

$$\vec{E}_r = |S_{21}|\vec{E}_I, \tag{13}$$

$$\vec{H}_r = |S_{21}|\vec{H}_I, \tag{14}$$

$$\eta = \frac{\frac{1}{2}|S_{21}|^2 \mathrm{Re}\iint \vec{E}_i \times \vec{H}_i d_s}{\frac{1}{2}\mathrm{Re}\iint \vec{E}_i \times \vec{H}_i d_s} = |S_{21}|^2. \tag{15}$$

Based on the results above, the MS efficiency can be improved effectively by improving the transmission coefficient; as a result, the Gain = D (directivity) × η can be improved. The comparison of gain of the MS with and without the cutting structure, at 2.4 GHz when the electromagnetic wave's direction is perpendicular to the MS, is shown in Figure 7. The peak gain of the MS with the cutting structure is 10.50 dBi, which is 2.04 dB higher than the peak gain without the cutting structure owing to the different S_{21}.

5 | TEST AND APPLICATION OF THE MS

The proposed MS is composed of 4 × 4 units, as shown in Figure 4A, and it is placed below the dielectric plate. These units are placed 3.17 mm aside from each other along the *X*-axis direction and 2.00 mm apart along the *Y*-axis direction. To verify circular polarization conversion, a source antenna operating at 2.4 GHz is designed. Considering its simple structure and easy of processing, the microstrip antenna is selected, as shown in Figure 8.

The microstrip antenna generates a linear polarized wave using coaxial line feeding. The feeding point (13, 4)

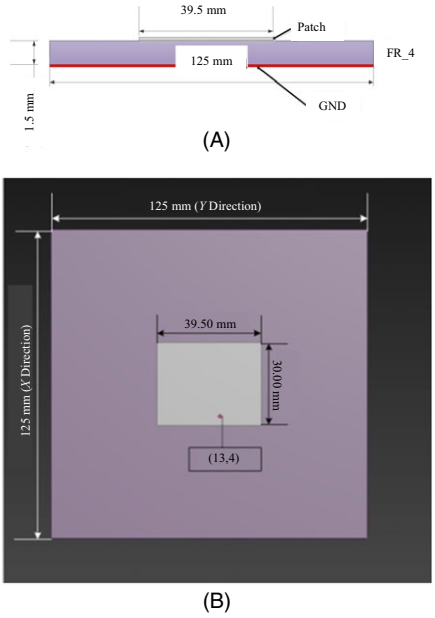

FIGURE 8 Geometry of the source antenna: (A) side view and (B) top view

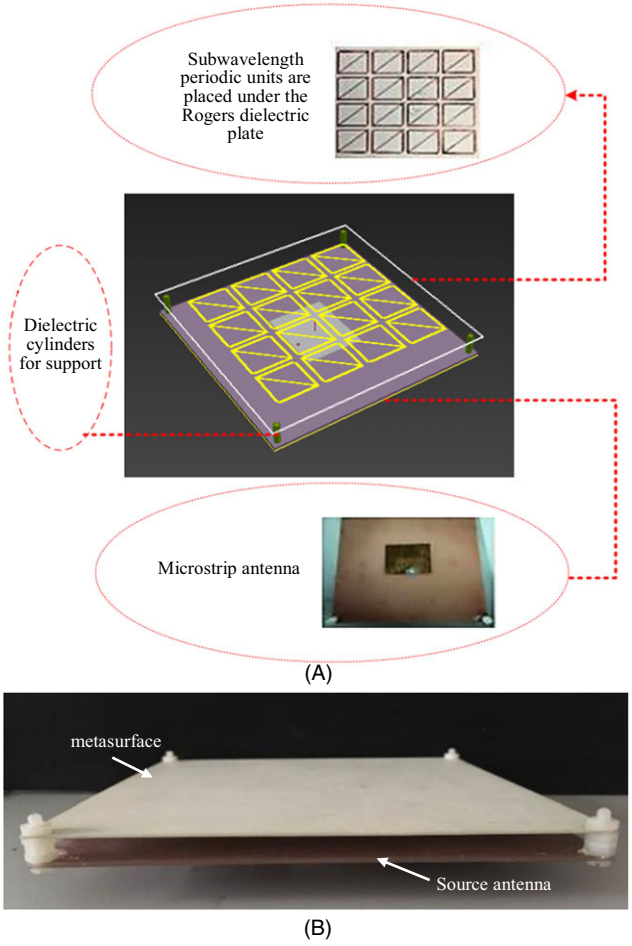

FIGURE 9 (A) Structure of the prototype; periodic units are below the Rogers dielectric plate and the source micro-strip antenna is under the MS; (B) Side view of the real verification model

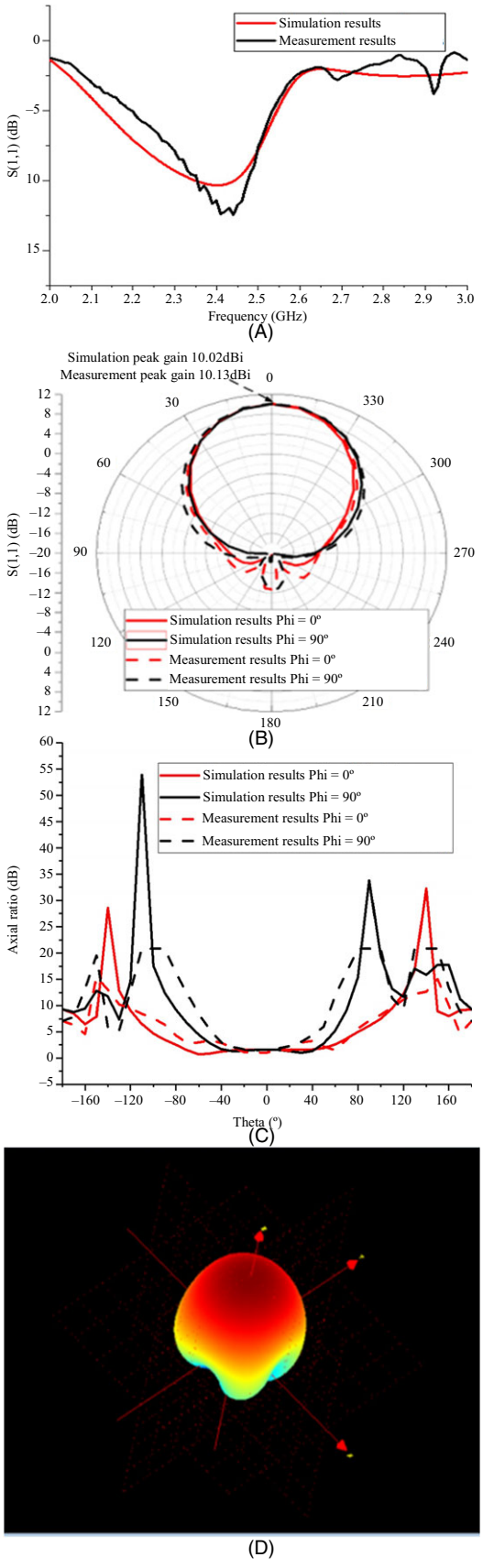

FIGURE 10 (A) Return loss of the antenna, (B) Gain at 2.4 GHz, (C) RHCP axial ratio at 2.4 GHz, and (D) Measurement result of 3-D pattern at 2.4 GHz

in mm is shown in Figure 8B. The size of the patch is 30 mm × 39.5 mm, printed at the center of the dielectric plate. The material of the dielectric is FR_4 ($\varepsilon_r = 4.48$, $\tan(\sigma) = 0.00321$) with a thickness of $H_1 = 1.5$ mm.

The verification model of the MS is shown in Figure 9. The MS is placed above the microstrip antenna, and it is supported by four dielectric cylinders. This verification system is simulated by a high-frequency structure simulator (HFSS) and measured using the SATIMO's Starlab system. The simulation and measurement results are in good agreement, as shown by Figure 10.

As shown in Figure 10A, the antenna operates at 2.4 GHz; the antenna exhibits a high gain when the MS is placed over the source antenna (Figure 10B). Figure 10C shows the polarization conversion of the antenna to circular polarization using the MS; the measurement results agree well with the simulation results within the main beam. Owing to SATIMO's measurement system, the axial ratio equal to or greater than 20 dB is displayed as 20 dB. Therefore, the maximum values for the measured results are 20 dB. The measurement result of the 3D pattern at 2.4 GHz is shown in Figure 10D to prove the smoothness of the pattern.

6 | CONCLUSIONS

The cavity mode theory is used to design MS by analyzing the electromagnetic wave propagation characteristics between the source antenna and the MS. Based on these analysis, we propose an MS can achieve polarization conversion. Furthermore, by introducing the cutting structure in MS, the electromagnetic phase difference between the incident and transmitted wave can be adjusted to −90°/90° from 1 GHz to 5 GHz. The proposed MS have circular polarization conversion functionality with a wider application operation bandwidth and higher gain than that of the previous structure. In addition, the proposed MS have potential applications in reconfigurable antennas and it will be carried out in the future.

ORCID

Aixin Chen http://orcid.org/0000-0003-3994-5848

REFERENCES

1. L. Zhang et al., *Adaptive decoupling using tunable metamaterials*, IEEE Trans. Microw. Theory Techn. **64** (2016), 2730–2739.
2. G. Minatti et al., *Synthesis of modulated-metasurface antennas with amplitude, phase, and polarization control*, IEEE Trans. Antennas Propag. **64** (2016), 3907–3919.
3. S. Wangand D. Gao, *Power transfer efficiency analysis of the 4-coil wireless power transfer system based on circuit theory and*

coupled-mode theory, IEEE Conf. Ind. Electron. Applicat. (ICIEA), Hefei, China, June 5–7, 2016, pp. 1230–1234.
4. Z. Song et al., *Broadband cross polarization converter with unity efficiency for terahertz waves based on anisotropic dielectric meta-reflectarrays*, Materials Lett. **159** (2015), 269–272.
5. Y. Guo et al., *Dispersion management of anisotropic metamirror for super-octave bandwidth polarization conversion*, Sci. Rep. **5** (2015), 8434:1–8434:7.
6. M. Pu et al., *Anisotropic meta-mirror for achromatic electromagnetic polarization manipulation*, Appl. Phys. Lett. **102** (2013), 131906:1–131906:4.
7. W. Chen, C. A. Balanisand C. R. Birtcher, *Checkerboard EBG surfaces for wideband radar cross section reduction*, IEEE Trans. Antennas Propag. **63** (2015), 2636–2645.
8. E. Carrascoand J. Perruisseau-Carrier, *Reflectarray antenna at terahertz using graphene*, IEEE Antennas Wireless Propag. Lett. **12** (2013), 253–256.
9. M. M. Islam, M. R. I. Faruque, and M. T. Islam, *A new metasurface based on meta-atom cluster for terahertz applications*, Microw. Opt Technol Lett **59** (2017), 2052–2057.
10. C. Murrayand R. R. Franklin, *Independently tunable annular slot antenna resonant frequencies using fluids*, IEEE Antennas Wireless Propag. Lett. **13** (2014), 1449–1452.
11. N. Rajakand N. Chattoraj, *A bandwidth enhanced metasurface antenna for wireless applications*, Microw. Opt Technol Lett. **59** (2017), 2575–2580.
12. H. X. Xu, G. M. Wang, and T. Cai, *Miniaturization of 3-D anistropic zero-refractive-index metamaterials with application to directive emissions*, IEEE Trans. Antennas Propag. **62** (2014), 3141–3149.
13. Y. M. Pan et al., *A low-profile high-gain and wideband filtering antenna with metasurface*, IEEE Trans. Antennas Propag. **64** (2016), 2010–2016.
14. K. L. Fordand K. Shah, *A study on the use of metasurface synthesis using electric and magnetic susceptibility*, *Loughborough Antennas Propag. Conf.* (LAPC), Loughborough, UK, Nov. 14–15, 2016, pp. 1–4.
15. Y. Zhou et al., *A microwave RCS reduction structure by antarafacial reflection design of gradient metasurface*, Progress Electromagn. Res. Symp. (PIERS), Shanghai, China, Aug. 8–11, 2016, pp. 4126–4130.
16. H. L. Zhu et al., *Linear-to-circular polarization conversion using metasurface*, IEEE Trans. Antennas Propag. **61** (2013), 4615–4623.

AUTHOR BIOGRAPHIES

Aixin Chen received his PhD degree in electromagnetic field and microwave technology from University of Electronic Science and Technology of China, Chengdu, China, in 1999. From 2000 to 2002, he was a postdoctoral fellow with the School of Electronic Information and Engineering, Beihang University, Beijing, China, where he is currently a professor. His research interests mainly include antennas and electromagnetic compatibility.

Xiangwei Ning received his BS degree from the School of Electronic and Information Engineering, Beihang University, Beijing, China, in 2016, and he is currently pursuing his MS degree in the same school. His main research interests include metasurface antenna, polarization conversion, and reconfigurable antenna.

Xin Liu received her BS degree from Xidian University in electronic information engineering in 2015 and MS degree from Beihang University in circuit and system in 2018. Her current research is reconfigurable antenna and circular polarization antenna.

Zhe Zhang received his BS and MS degrees in electrical engineering from Nanjing University of Aeronautics and Astronautics, Nanjing, China, and Lanzhou University, Lanzhou, China, in 2012 and 2016, respectively. He is currently pursuing PhD degree in the School of Electronics and Information Engineering, Beihang University, Beijing. His current research interests include metamaterials-based antenna and airborne antenna.